International Journal of Computational and Experimental Science and ENgineering (IJCESEN)

Vol. 11-No.4 (2025) pp. 7887-7896
http://www.ijcesen.com

ISSN: 2149-9144

Research Article

Density Functional Theory Analysis of Structural and Electronic Properties of IV–VI Semiconductors: PbSe, PbS, and $PbSe_xS_x$ Alloys

Yamina Benkrima[1*], Yousra Megdoud[2], Mosbah Laouamer[3], Redha Meneceur[4], Mohammed Khadem [5]

[1] Ecole Normale Superieure de Ouargla 30000 Algeria.
* **Corresponding Author Email:** benkrima.yamina@ens-ouargla.dz - **ORCID:**0000-0002-7089-7904

[2]Institute of Sciences, University Center of Tipaza, Algeria
Email: y.megdoud23@gmail.com **ORCID:** 0009-0004-9609-3658

[3]UDERZA Unit, Faculty of Technology, University of El Oued, 39000 El Oued, Algeria.
Email: mosba2h@gmail.com - **ORCID:** 0000-0002-5247-7004

[4]UDERZA Unit, Faculty of Technology, University of El Oued, 39000 El Oued, Algeria.
Email: redh2a@gmail.com - **ORCID:** 0000-0002-5247-70003

[5]DIMEG, University of Calabria, Rende (CS).87036 Italy
Email: khade2m@gmail.com - **ORCID:** 0000-0002-5247-7002

Article Info:

DOI: 10.22399/ijcesen.4164
Received : 08 June 2025
Accepted : 24 September 2025

Keywords

FP-LAPW,
DFT,
semiconductors,
electronic structure,
optical absorption.

Abstract:

This study presents first-principles calculations performed within the framework of density functional theory (DFT) using the full-potential linearized augmented plane wave (FP-LAPW) method as implemented in WIEN2k. Exchange–correlation interactions are described through the Wu–Cohen generalized gradient approximation (WC-GGA), while the modified Becke–Johnson (mBJ) potential is applied to improve the accuracy of the electronic band gap. The analysis initially focuses on the structural and electronic properties of PbS and PbSe in their NaCl-type phase. The results confirm that both compounds exhibit a direct band gap located at the L point. The investigation then extends to the ternary $PbSe_{1-x}S_x$ alloys, where the influence of composition on lattice parameters and bulk modulus is systematically examined. The findings reveal clear deviations from Vegard's law, interpreted within the theoretical framework proposed by Zunger and co-workers. Furthermore, the dependence of the band gap on alloy composition is analyzed under different pressure conditions. In addition to electronic properties, the optical response is also explored, including the dielectric function, refractive index, absorption coefficient, and reflectivity, highlighting the potential of these materials for optoelectronic and photovoltaic applications.

1. Introduction

Lead chalcogenides, particularly PbS and PbSe, have become the subject of intensive research owing to their remarkable combination of structural, electronic, optical, and thermoelectric properties. These IV–VI semiconductors crystallize in the rocksalt (NaCl) structure [1] and are characterized by narrow direct band gaps, strong infrared absorption, and high carrier mobility. Such attributes make them highly attractive for infrared detection, optoelectronic applications, and thermoelectric energy conversion. Alloying represents a widely adopted strategy to tailor these intrinsic properties, enabling fine-tuning of electronic and structural features. In this context, ternary alloys such as $PbSe_{1-x}S_x$ allow continuous adjustment of lattice constants, band-gap energies, and absorption edges, thereby improving device efficiency and thermoelectric performance.Previous first-principles studies have explored $PbSe_{1-x}S_x$ and related alloys, including $PbSe_{1-x}Te_x$ and $PbS_{1-x}Te_x$ [2]. These works reported nonlinear variations in lattice constants, bulk modulus, and band-gap

behavior, as well as analyses of miscibility, bowing parameters, and phase stability. Despite these efforts, conventional density functional theory (DFT) methods—such as the local density approximation (LDA) and generalized gradient approximation (GGA)—are well known for underestimating experimental band gaps and providing limited accuracy in reproducing optical spectra [3,4]. This limitation underscores the importance of employing more advanced exchange–correlation functionals for reliable band-structure predictions.In addition, the combined effect of external pressure and alloy composition on electronic structure and optical responses remains insufficiently explored. Parameters such as the dielectric constant, refractive index, reflectivity, and absorption are strongly dependent on both composition and pressure, yet few studies have systematically addressed these influences. A deeper understanding of these interrelated effects is essential, as they directly determine the suitability of these materials for practical applications in optoelectronics, photovoltaics, and thermoelectric devices.Motivated by these considerations, the present work undertakes a comprehensive theoretical study of the structural, electronic, and optical properties of PbS, PbSe, and their ternary alloys $PbSe_{1-x}S_x$. The calculations are carried out using the full-potential linearized augmented plane wave (FP-LAPW) approach within the WIEN2k package. To enhance the accuracy of electronic structure predictions, particularly the band gap, the modified Becke–Johnson (mBJ) functional is applied in addition to the Wu–Cohen GGA. The analysis emphasizes the influence of alloy composition and pressure on material properties, with special focus on deviations from Vegard's law and on the determination of key optical quantities—namely the dielectric function, refractive index, absorption coefficient, and reflectivity—that are critical for the development of next-generation optoelectronic devices.

2. Computational Details

The present investigation makes use of the full-potential linearized augmented plane wave (FP-LAPW) technique **[5],** realized in the WIEN2k package **[6],** within the framework of density functional theory (DFT) **[7,8].** The study addresses the structural, electronic, and optical properties of the binary semiconductors PbS and PbSe, together with their ternary alloy $PbSe_{1-x}S_x$. Structural optimization was performed using the Wu–Cohen generalized gradient approximation (WC-GGA) **[9]** for the exchange–correlation potential, while the modified Becke–Johnson (mBJ) potential **[10]** This approach is used to refine the description of the electronic structure, especially the band gap, since conventional DFT is known to systematically underestimate energy gaps. Within the FP-LAPW scheme, the crystal volume is divided into non-overlapping atomic spheres (muffin-tin regions) and an interstitial region. Inside the muffin-tin spheres, wave functions, electron densities, and potentials were expanded in spherical harmonics up to lmax = 10, whereas plane-wave expansions with a Fourier cutoff defined by RMT•Kmax = 8 were used in the interstitial region. Here, RMT represents the smallest muffin-tin radius, while Kmax corresponds to the largest reciprocal lattice vector included in the expansion. The muffin-tin radii were chosen as 2.0 a.u. for Pb, Se, and S atoms. A separation energy of –6 Ry was used to distinguish between core and valence states. Convergence of the self-consistent cycle was reached when the change in total energy between successive iterations became smaller than 0.1 mRy.In our calculations, we take into account the following electronic configuration:

Pb: [**Xe]** $6s^2\ 4f^{14}\ 5d^{10}\ 6p^2$

Se: [Ar] $3d^{10}\ 4S^2\ 4p^4$

S: [Ne] $3S^2\ 3P^4$.

3. Results and discussions

3.1 Structural Analysis

In our computational approach, particular importance is given to the determination of structural parameters, as they constitute the foundation for investigating other physical properties of solids. The key parameters include the equilibrium lattice constants (a_0, b_0, c_0), the bulk modulus (B_0), and its pressure derivative (B_0'). These quantities can be obtained either experimentally, primarily through X-ray diffraction (XRD), or theoretically via ab initio simulations. In this study, we employed the latter strategy using the WIEN2k package. The full energy was computed for a series of unit cell volumes, and the equilibrium structural parameters were extracted from the resulting energy–volume relationship. Specifically, the calculated Etot(V) data were close-fitting to the Murnaghan equation of state [11], which can be expressed as:

$$E(V) = \frac{B_0 V}{B_0'}\left[\frac{(V_0/V)^{B_0'}}{B_0'-1} - 1\right] + E(V_0) - \frac{B_0 V}{B_0'-1} \quad \textbf{(1)}$$

where:

E(V) represents the total ground-state energy in relation to the unit-cell volume V

V.B_0 is the equilibrium bulk modulus,

V_0 is the equilibrium volume, and

B_0' is the first derivative of the bulk modulus with respect to pressure.

The equilibrium lattice parameters were obtained from the minimum of the Etot V curve. The bulk modulus B_0 was extracted from the relation:

$$B_0 = V\frac{\partial^2 E}{\partial V^2} \qquad (2)$$

This procedure was applied to the binary compounds PbSe and PbS in order to determine their most stable phase and structural parameters.The results indicate that these compounds stabilize in the NaCl-type (B1) crystal structure under standard conditions (T = 0 K, P = 0 GPa), consistent with earlier theoretical and experimental reports. The calculated structural parameters including the lattice constant (a), bulk modulus (B), and its pressure derivative (B′) are listed in Table 1 alongside corresponding literature values. The slight discrepancies observed between computed and experimental lattice constants are attributed to the choice of the WC-GGA functional. For phases where experimental measurements are not available, the present outcomes show good agreement with previous theoretical studies. The structural investigation is also extended to the ternary $PbSe_{1-x}S_x$ alloy system.Figure 1 presents the total energy as a function of unit cell volume for the ternary alloys at concentrations x = 0.25, 0.5, and 0.75, obtained within the WC-GGA approximation for the NaCl (B1) phase. These results provide valuable information regarding the stability of the alloyed systems, confirming that the equilibrium structure of the parent compounds, PbSe and PbS, also corresponds to the NaCl (B1) configuration.For the ternary alloys, the atomic positions were modeled within the B1 (NaCl-type) structure as a representative configuration. The equilibrium lattice constants and bulk moduli were determined by fitting the calculated energy–volume data to the Murnaghan equation of state and then compared with available theoretical and experimental reports. Furthermore, the evolution of the lattice constant as a function of composition was examined in the context of Vegard's law [15], which assumes a linear dependence of the lattice parameter on the alloy concentration x:

$$a\,(A_xB_{1-x}C) = x a_{AC} + (1-x)a_{BC} \qquad (3)$$

Here, a_{AC} refers to the lattice constant of compound AC, while a_{BC} corresponds to that of compound BC.. In real systems, however, deviations from the ideal Vegard's law behavior are frequently encountered, giving rise to positive or negative bowing relative to the linear interpolation. As illustrated in **Fig. 2**, our results show that the equilibrium lattice constants of $PbSe_{1-x}S_x$ exhibit an almost linear dependence on composition, with a small bowing parameter of –0.701. This slight deviation can be accredited primarily to the lattice divergence between the two parent compounds. Figure 3 further depicts the variation of the bulk modulus as a function of alloy composition x.Although the bulk modulus of $\mathbf{PbSe_{1-x}S_x}$ alloys generally follows a linear concentration dependence (LCD), noticeable deviations were identified, characterized by a bowing parameter of **59.701** GPa. This deviation originates mainly from the disparity in bulk modulus values between the two parent compounds. In general, the bulk modulus decreases progressively with increasing sulfur content, reflecting an enhancement in the compressibility of the ternary alloys.

3.2 Electronic Analysis

The present section discusses, we report the results of the electronic assembly calculations for the binary compounds **PbSe** and **PbS**, as well as their ternary alloy $\mathbf{PbSe_{1-x}S_x}$**.** The band structures were evaluated along the high-symmetry paths of the first Brillouin zone using both the WC-GGA and the modified Becke–Johnson (mBJ) formalisms, based on the optimized lattice parameters obtained from the structural analysis. For the binary compounds, which crystallize in the NaCl-type cubic phase, the calculated band structures confirm that PbSe and PbS are direct band-gap semiconductors with transitions located at the Γ point **(Γ → Γ),** as shown in **Fig. 4.** The mBJ-derived band gaps align well with the values reported in experimental studies and previous theoretical calculations.While a slight underestimation with respect to experimental results persists a well-documented limitation of density functional theory when applied to semiconductors and insulators **[16–25]** the mBJ approach offers a significant improvement over WC-GGA and other standard approximations. In certain cases, the band gaps predicted by mBJ are marginally larger than experimental values but remain within the range of previously reported theoretical estimates. These results underline the effectiveness of the mBJ potential in providing more accurate band-gap predictions for semiconductors such as PbSe and PbS, thereby

serving as a reliable correction to the systematic deficiencies of conventional DFT calculations.The electronic band structures of $PbSe_{1-x}S_x$ ternary alloys were examined for compositions x=0.25,0.50, and 0.75 in their most stable phase. Calculations were carried out along the main high-symmetry directions of the Brillouin zone using both the WC-GGA and mBJ schemes. The primary aim of this analysis is to investigate how the energy band gap evolves with alloy composition. A summary of the calculated results is provided in Table 5. For the binary end members, the band-gap values obtained with the mBJ potential show strong consistency with experimental observations, thereby confirming the reliability of this functional in predicting alloy band gaps. In contrast, the compositional dependence of the band gap does not follow a simple linear Vegard-like trend. Rather, it is more accurately represented by a quadratic expression of the form:

$$E_{gABC} = xE_{gAC} + (1-x)E_{gAB} \qquad (4)$$

The parameter b, known as the bowing coefficient, characterizes the extent of deviation from linearity. Such non-linear variations are commonly encountered in semiconductor alloys and arise mainly from lattice mismatch and chemical disorder between the constituent compounds.

Effect of Bowing in $PbSe_{1-x}S_x$

The band gaps determined using the WC-GGA and mBJ exchange–correlation techniques for the studied $PbSe_{1-x}S_x$ alloys show a noticeable bending trend. By fitting the computed values to a quadratic function, the composition dependency of the band gap was examined, and the resulting relations are as follows:

$$E_g^{WC-GGA} = 0.413 - 0.336X + 0.459X^2$$

$$E_g^{mBj} = 1.081 - 0.295X + 0.495X^2$$

These results demonstrate how important the bending parameter is for describing the electrical properties of $PbSe_{1-x}S_x$ alloys. The differences in the parent compounds' intrinsic band gaps and lattice characteristics are primarily responsible for the observed departure from linearity. For optoelectronic and photovoltaic devices, where precise band-gap adjustment is a crucial prerequisite for performance optimization, an understanding of such bowing effects is especially relevant.

1.1. Optical Analysis

Since semiconductors play a vital part in modern electronic and optoelectronic applications, their optical responsiveness is extremely important. The interaction between electromagnetic radiation and the semiconductor material, especially when exposed to external excitation like input photons, is what causes these reactions. This interaction manifests itself in several ways, including absorption, reflection, refraction, transmission, scattering, and emission. The study of the complex dielectric function in a quantum-mechanical context and its relationship to the refractive index via the Kramers–Kronig relations are essential for a thorough comprehension of these phenomena.

A- Dielectric Function

The frequency-dependent dielectric function is expressed as:

$$\varepsilon_2(\omega) = \frac{4\pi^2 e^2}{m^2\omega^2}\sum_{i,j}|\langle i|M|j\rangle| * f_i(1 - f_i(\omega) - h\omega)d^3k \qquad (5)$$

where $rM_{cv}(k) = \langle u_{ck}|e\nabla|u_{vk}\rangle$ **[26]** designate the real and imaginary components, respectively. The imaginary component, M_{cv} (k), is intrinsically connected to the electrical band structure and delineates the optical absorption resulting from interband transitions. The momentum matrix elements between occupied and unoccupied electronic states can be derived as follows:

$$\varepsilon_1(\omega) = 1 + \frac{2}{\pi}P\int_0^\infty \frac{\varepsilon_2(\omega')\omega' d\omega'}{\omega'^2 - \omega^2} \qquad (6)$$

The real part, $\varepsilon_1(\omega)$is derived from using the Kramers–Kronig transformation

B- Refractive Index

An important related optical constant is the complex refractive index, expressed as:

$$n(\omega) = \frac{1}{\sqrt{2}}\left[\sqrt{\varepsilon_2^2(\omega) + \varepsilon_2^2(\omega)} + \varepsilon_1(\omega)\right]^{1/2} \qquad (7)$$

At zero frequency, this expression reduces to the static refractive index n(0), which can also be correlated to the static dielectric constant ($\omega = 0$). Several semi-empirical models (e.g., Ravindra, Herve–Vandamme, Reddy–Nazeer) **[26]** relate the refractive index to the fundamental band gap and electronegativity differences, offering useful predictive schemes for comparison with first-principles results.

C- Absorption Coefficient

The absorption coefficient α(ω) measures the proportion of energy absorbed per unit length within the material. It is connected to the extinction coefficient and dielectric function via:

$$\alpha(\omega) = \frac{4\pi}{\lambda} k(\omega) \qquad (8)$$

A pronounced absorption onset is associated with the fundamental optical transition across the band gap, a key parameter for evaluating the suitability of these materials as absorbers in photovoltaic and optoelectronic devices. The optical response was calculated using the WIEN2k package within the framework of density functional theory. Following the self-consistent determination of the electronic ground state (SCF cycle), the optical spectra were obtained through the Optic, Joint, and Kram modules. Calculations were carried out within the WC-GGA approximation, while the modified Becke–Johnson (mBJ) potential was additionally employed to achieve a more accurate description of the band gaps. To properly capture the interband transitions, a dense k-point sampling of 600 points in the Brillouin zone was adopted.The optical spectra were computed over a wide photon-energy range, extending from 0 to 40 eV, thus encompassing the infrared, visible, and ultraviolet regions. The absorption edge appears at 0.547 eV for PbSe and 0.231 eV for PbS, both corresponding to direct optical transitions. The dominant absorption peaks are located at 4.239 eV for PbSe and 5.563 eV for PbS, originating from intense interband transitions involving deeper valence and higher conduction states **(Fig. 5).**The refractive index spectra display distinct peaks at 1.903 eV for PbSe and 5.36 eV for PbS. The corresponding static refractive indices $n(0)$ were also determined from the low-energy limit of the spectra. The reflectivity profiles reveal moderate values, with maxima of 64% for PbSe at 8.91 eV and 65% for PbS at 10.12 eV. These pronounced features in the ultraviolet region suggest that both compounds could serve as promising candidates for UV optical coatings (Fig. 6).For the alloy compositions x = 0.25, 0.50, and 0.75, the fundamental absorption edges are located at 0.224, 0.432, and 0.709 eV, respectively (Fig. 7). These thresholds correspond to direct inter b and electronic transitions. The real component of the dielectric function has a distinctive dispersive pattern, with zero-crossings occurring between 4.55 and 4.75 eV, indicating the photon energies linked to peak absorption. The maximum values of the refractive index are found at 2.007 eV for x = 0.25, 2.613 eV for x = 0.50, and 3.0 eV for x = 0.75, clearly reflecting the compositional dependence of the alloys (Fig. 8). The progressive increase in the refractive index peak with higher sulfur content indicates enhanced electronic transitions, which can be attributed to the widening of the band gap.The absorption edge exhibits a clear compositional dependence, shifting from 0.276 eV at x = 0.25 to 0.441 eV at x = 0.50, and 0.536 eV at x = 0.75. The maximum absorption intensities are observed in the range of 6.3–6.8 eV (Fig. 9), underscoring the pronounced optical activity of these alloys in the ultraviolet region. A reflectivity spectra of $PbSe_{1-x}S_x$ alloys exhibit maxima of 62.7%, 61.5%, and 63.7% at photon energies of 8.20 eV, 8.18 eV, and 8.00 eV, respectively (Fig. 10). These results demonstrate that the alloys preserve the high ultraviolet reflectance characteristic of the parent binaries, while simultaneously providing compositional tunability of the optical response.A detailed analysis of the optical characteristics of PbSe, PbS, and their ternary alloys $PbSe_{1-x}S_x$ reveals several noteworthy results. All studied compounds display direct optical transitions at the Brillouin zone center, a property that is particularly beneficial for optoelectronic devices such as infrared detectors and solar absorbers. The pronounced band-gap bowing observed in the alloys allows precise adjustment of the absorption edge, demonstrating the flexibility of $PbSe_{1-x}S_x$ systems for tunable applications. In addition, the strong absorption and reflectivity peaks in the ultraviolet region suggest potential uses in UV photonics and protective optical coatings. The

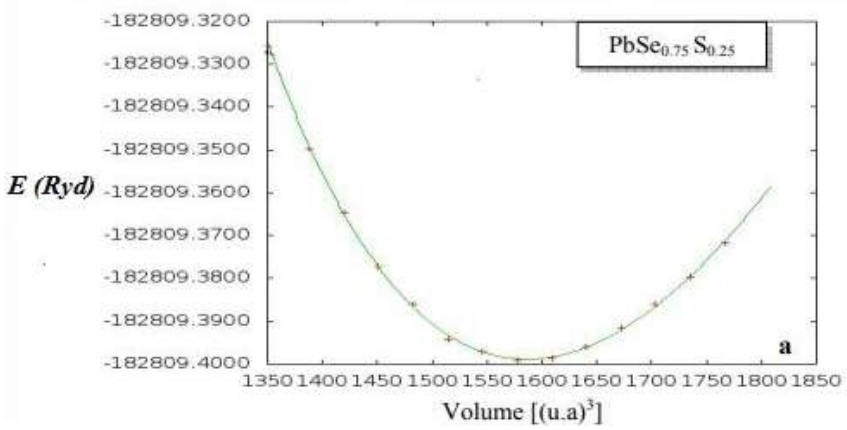

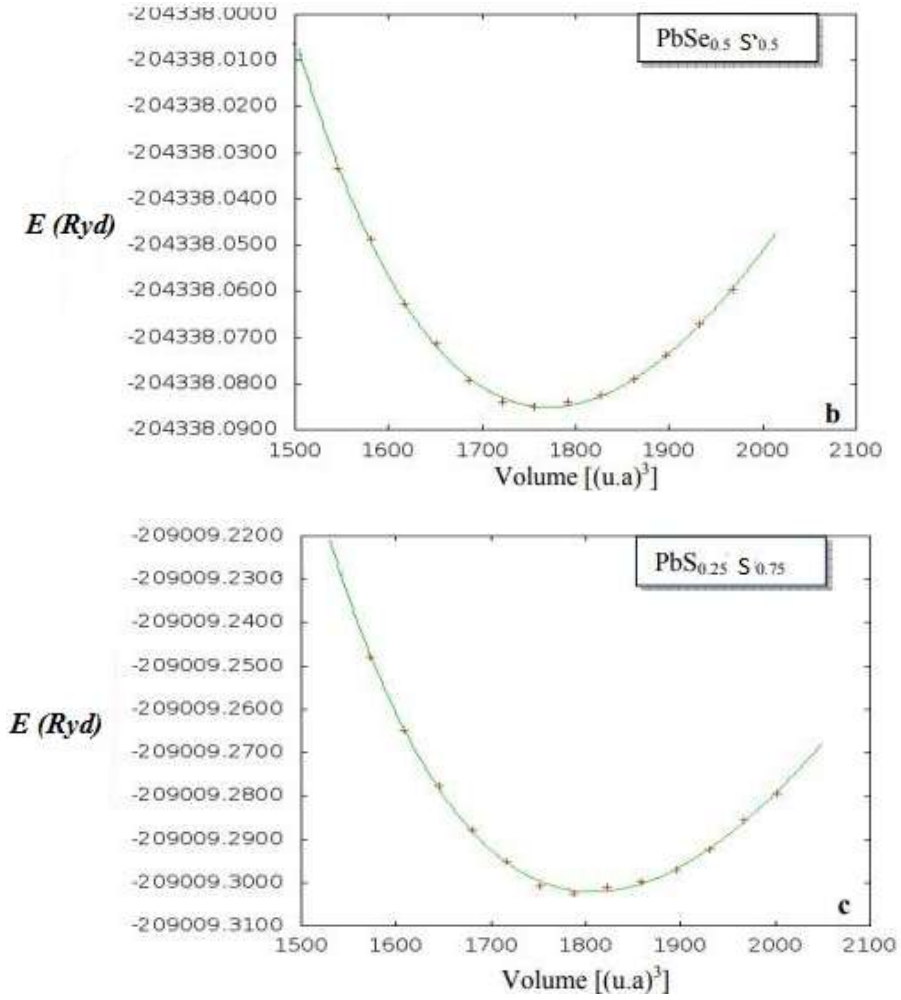

Figure 1. *Variation of total energy with respect to cell volume for $PbSe_{1-x}S_x$ at x=0.25,0.50, and 0.75, calculated within the NaCl-type structure.*

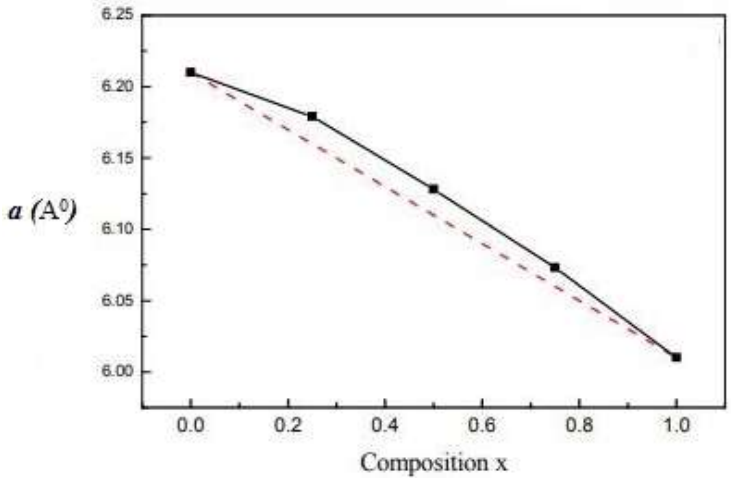

Figure 2. *Variation of the lattice constraint as a function of meditation for $PbSe_{1-x}S_x$ (solid line), compared with that obtained from Vegard's law (dashed line).*

Table 1. *The calculated lattice parameters (Å), bulk modulus (GPa), and first pressure derivatives for $PbSe_{1-x}S_x$ alloy phases are provided.*

Alliages / $PbSe_{1-x}S_x$		a (A^0)		B(GPa)	B'
	Our calculs	0.25	6.179	46.783	4.52

		0.5	6.128	47.462	4.31
		0.75	6.073	49.211	4.01
	Other calculs	0.25	6.174[a]	48.2[a]	-
		0.5	6.122[b]	47.462[b]	-
		0.75	6.069[c]	49.211[c]	-

[a]Ref[12], [b]Ref [13], [c]Ref [14].

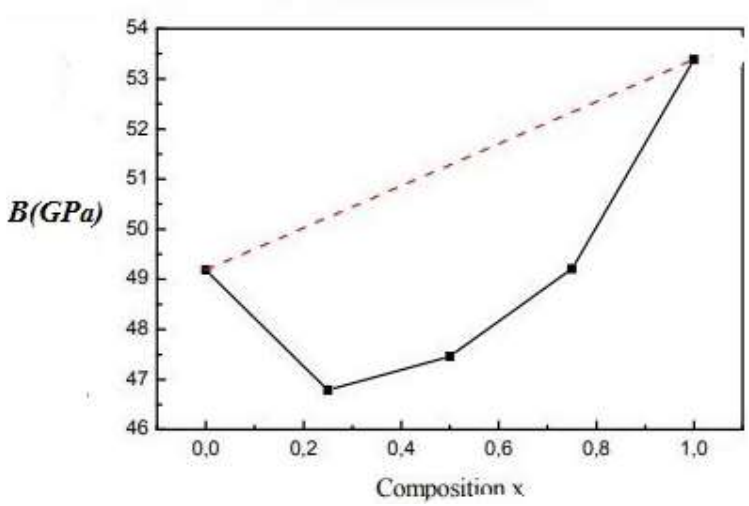

Figure 3. *Variation of the bulk modulus as a function of concentration for $PbSe_{1-x}S_x$ (solid line), compared with that obtained from the linear concentration dependence law (dashed line).*

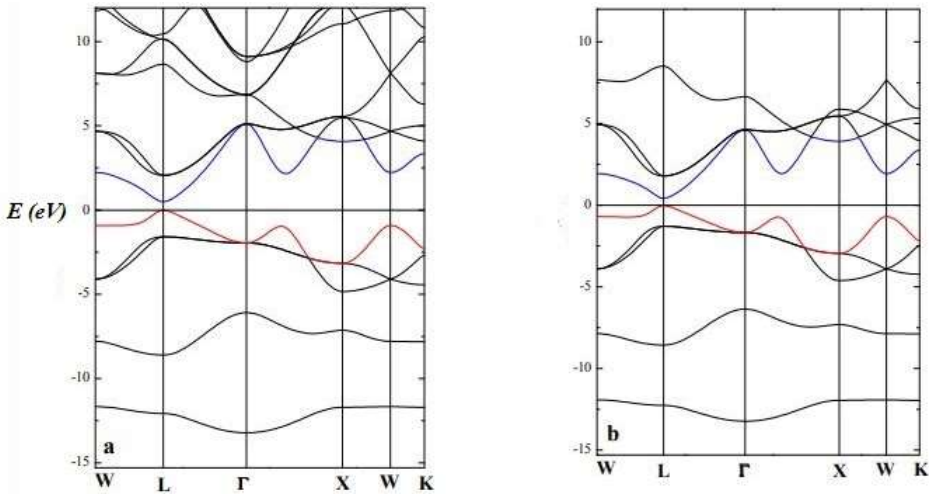

Figure 4*. Band structure of PbSe (a) and PbS (b) calculated using the WC-GGA approximation.*

Table 2. *Gaps and Energy of the binary compounds PbSe and PbS.*

	Nos Calculs	Autre Calculs
	WC-GGA mBj	
PbSe	0.425 1.099	0.340[a] 0.318[b] 0.295[c]
PbS	0.496 1.248	0.380[a] 0.448[b]

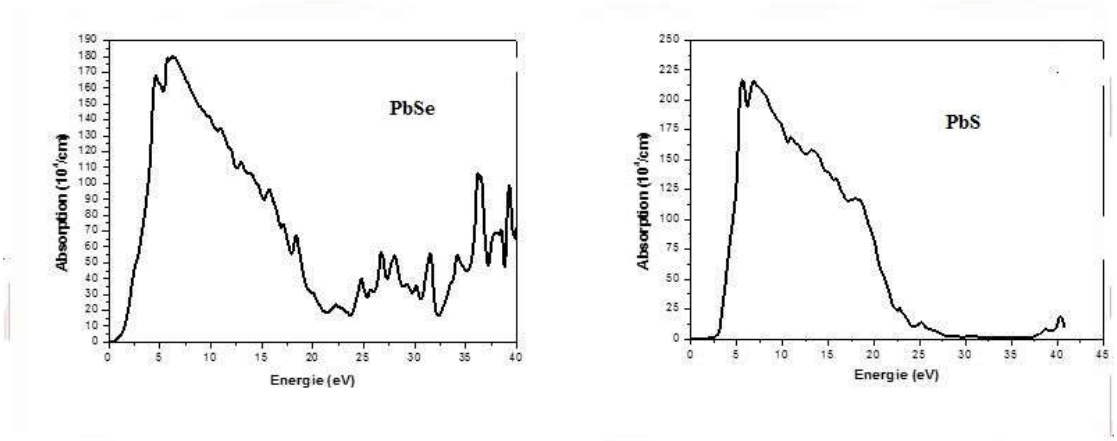

Figure 5. *Absorption variation as a function of energy for PbSe and PbS.*

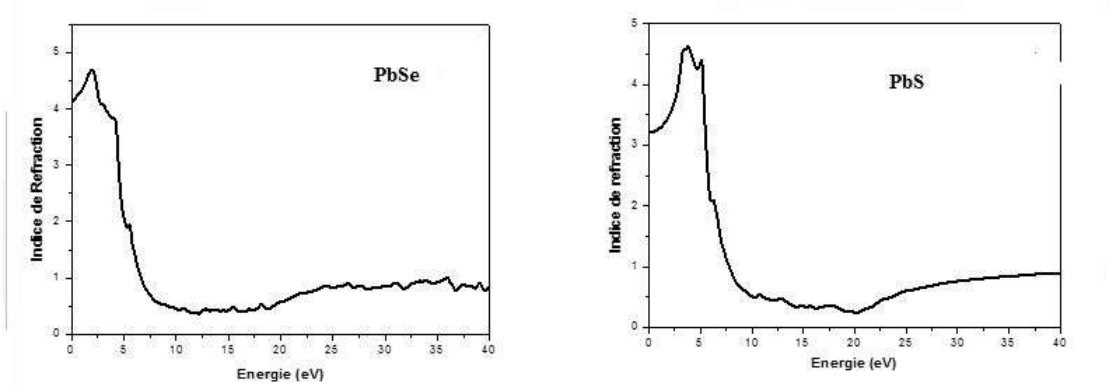

Figure 6. *Variation of the refractive index as a function of energy for lead selenide and lead sulfide.*

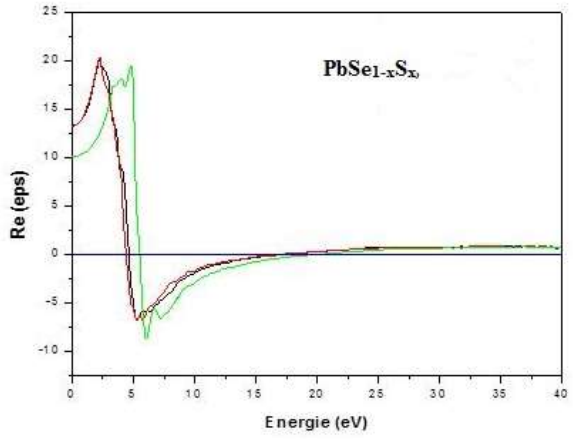

Figure 7*. Fluctuation of the real component of the dielectric function as a function of energy for PbSe and PbS.*

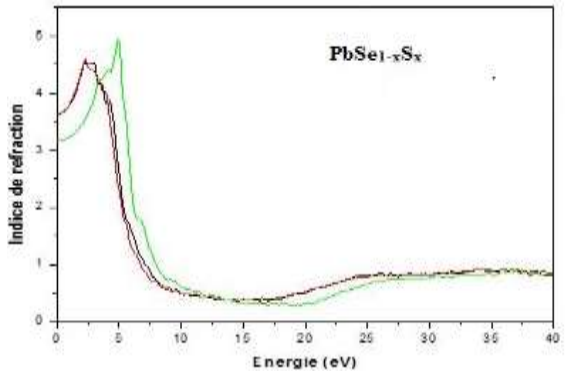

Figure 8. *Energy-dependent variation of the refractive index for PbSe and PbS*

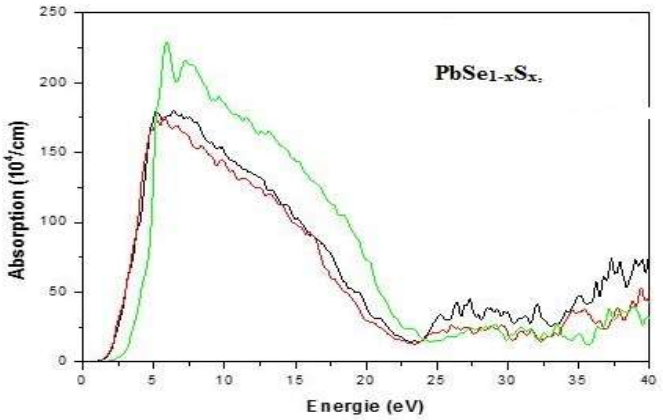

***Figure 9**. Energy-dependent absorption spectra of PbSe and PbS*

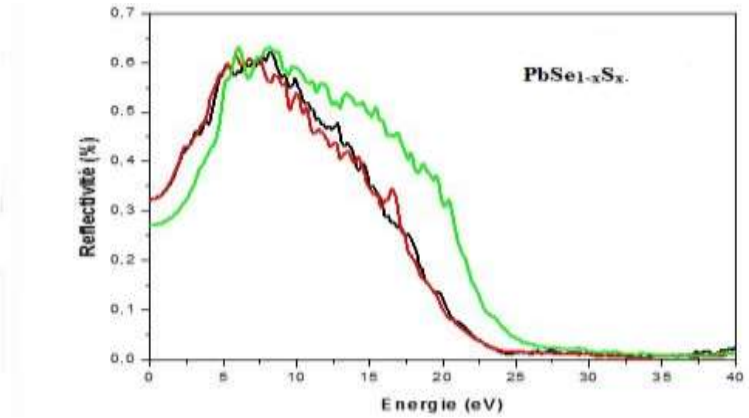

***Figure 10.** Variation in reflectance as a function of energy for $PbSe_{1-x}S_x$.*

consistency between the calculated and experimental static optical parameters further validates the reliability of the WC-GGA combined with the mBJ potential in accurately capturing the optical response of these semiconductors.

4. Conclusions

This study provides a comprehensive analysis of the structural, electronic, and optical properties of the binary semiconductors PbSe and PbS, together with their ternary alloys $PbSe_{1-x}S_x$, employing the ab initio full-potential linearized augmented plane wave (FP-LAPW) method within the density functional theory (DFT) framework. The optimized lattice parameters and bulk modulus show close agreement with available theoretical and experimental data, validating the robustness of the computational approach. Band-structure simulations confirm that all compounds act as direct band-gap semiconductors, with the WC-GGA and mBJ formalisms producing gap values that are consistent with prior theoretical studies and reasonably close to experimental measurements. Particular emphasis is placed on the dielectric function and refractive index, which play a decisive role in optoelectronic performance; the calculated spectra reproduce the key features reported in earlier investigations, thereby strengthening the reliability of the present findings. Overall, the results demonstrate that PbSe, PbS, and their $PbSe_{1-x}S_x$ alloys possess tunable band gaps and favorable optical responses, making them promising candidates for a wide range of optoelectronic applications, including photodetectors, solar absorbers, and ultraviolet protective coatings.

Author Statements:

- **Ethical approval:** The conducted research is not related to either human or animal use.
- **Conflict of interest:** The authors declare that they have no known competing financial interests or personal relationships that could have appeared to influence the work reported in this paper

- **Acknowledgement:** The authors declare that they have nobody or no-company to acknowledge.
- **Author contributions:** The authors declare that they have equal right on this paper.
- **Funding information:** The authors declare that there is no funding to be acknowledged.

- **Data availability statement:** The data that support the findings of this study are available on request from the corresponding author. The data are not publicly available due to privacy or ethical restrictions.

References

[1] S. H. Wei, H. Krakauer, Phys. Rev. Lett. 55, 1200 (1985)

[2] G.A. Baraff, M. Schülter, Phys. Rev. B 30, 3460 (1981)

[3] M. Lannoo, M. Schülter, L.J. Sham, Phys. Rev. B 32, 3890 (1984)

[4] L.K. Teles, J. Furthmuller, L.M.R. Scolfaro, J.R. Leite, F. Bechstedt, Phys. Rev. B 62, 2475 (2000)

[5] M.A. Blanco, A. Martín Pendás, E. Francisco, J.M. Recio, R. Franco, J. Mol. Struct.Theochem.368, 245 (1996).

[6]P. Blaha, K. Schwarz, G. K. H. Madsen, D. Kvasnicka, J. Luitz, WIEN2K, An Augmented Plane Wave Plus Local Orbitals Program for Calculating Crystal Properties, Vienna University of Technology, Austria, 2001.

[6] P. Hohenberg and W. Kohn, Phys. Rev. 136, B864 (1964)

[7] W. Kohn L.J. Sham, Phys. Rev. 140, B1133 (1965)

[8] F. D. Murnaghan, Proc. Natl. Acad. Sci. USA 30, 5390 (1944)

[9] J.P. predew, K. Burke and M. Ernzerhof, Phys. Rev. Lett. 77, 3865 (1996)

[10] B.K. Agrawal, S. Agrawal, P.S. Yadav, and S. Kumar, J. Phys.: Condens. Matter 9, 1763 (1997).

[11] J.S. Almeida and R. Ahuja, Appl. Phys. Lett. 89 61913 (2006)

[12] R. Miloua, Z. Khebbab, F. Miloua, N. Benramdane, Phys. Lett. A372, 1910 (2008)

[13]O. Madelung, M. Schulz, H.Weiss (Eds), Numerical Data and Functional Relationships in Science and Technology Landolt-Bornstei, New Series, vol. 17, Springer, Berlin, 1983

[14] M.L. cohen, J.R. chelkowsky, Electronic Structure and Optical Properties of Semiconductors, second ed, Springer Series in Solid States Sciences,vol.75, Springer-Verlag, Berlin, 1989.

[15] M.Lach-hab, A.D. Papaconstantopoulos, J.M. Mehl, J. Phys. Chem. Solids 63,833 (2002)

[16] S. Wei, A. Zunger, Phys.Rev. B55, 13605 (1997)

[17] A. Zaoui and F. El Haj Hassan, J. Phys.: Condens. Matter 13, 253 (2001)

[18] Kacimi S, Zaoui A, Abbar B and Bouhafs B J. Alloys Compounds 462 135(2008).

[19] R Dalven, Ehrenreich H, Seitz F and Turnbull D (ed) Solid State Physics vol 28 p 179 (1973).

[20] L. Vegard, Z. Phys, 517 (1921)

[21] E.A. Albanesi, C.M.I. Okoye, C.O. Rodriguez, E.L. Peltzer, Y. Blanca, A.D. Petukhov, Phys. Rev. B 61, 16589 (2000).

[22] P. Dufek, P. Blaha, K Schwarz, Phys. Rev. B 50, 7279 (1994)

[23] G.B. Bachelet, N.E. Christensen, Phys. Rev. B31, 879 (1995)

[24] E. Engel, S.H. Vosko, Phys. Rev. B 47, 13164 (1993)

[25] A. Zaoui, S. Kacimi, M. Zaoui, B. Bouhafs, Materials Chemistry and Physics 114, 650 (2009)

[26] Z. Charifi, H. Baaziz, N. Bouarissa, Int. J. Mod. Phys. B18, 137 (2004)

[27] J. Van Vechten and T.K. Bergstresser, Phys. Rev. Lett. 31, 3351 (1970)

[28] J.E. Bernard and A. Zunger, Phys. Rev. Lett. 34, 5992 (1986)

[29] Z. Nabi, B. Abbar, S. Meçabih, A. Khalfi, N. Amrane, Comput.mat.sci, 18, 127 (2000)

[30] G. Nimtz, B. Schlicht, Narrow-gap Semiconductors, Springer, New Work, (1985)